# Properties of Fiber-Reinforced Alkali-Activated Concrete (FRAAC)

**Arkamitra Kar, Pujitha Ganapathi Chottemada, Lucija Hanžič, Sri Kalyana Rama Jyosyula, Patricia Kara De Maeijer, Behzad Nematollahi, Kruthi Kiran Ramagiri, Laura Rossi, Aljoša Šajna, Shizhe Zhang, Mingzhong Zhang, Guang Ye, and Frank Dehn**

**Abstract** The use of fibers to address tensile cracking in alkali-activated concrete (AAC) is a topic of ongoing research. The addition of fibers enhances the tensile and flexural characteristics of all types of concrete including AAC. However, the mixing process, the setting time, and the workability are compromised due to the presence of fibers in the hardened matrix. There are different material categories of fibers such as steel, synthetic, carbon, and organic fibers that can impart different

A. Kar (✉) · P. Ganapathi Chottemada
Department of Civil Engineering, Birla Institute of Technology and Science (BITS)-Pilani, Hyderabad Campus, Hyderabad, Telangana, India
e-mail: arkamitra.kar@hyderabad.bits-pilani.ac.in

L. Hanžič · A. Šajna
Zavod Za gradbeništvo (ZAG) Slovenije, Slovenian National Building and Civil Engineering Institute, Ljubljana, Slovenia

S. K. R. Jyosyula
Department of Civil Engineering, Mahindra University, Hyderabad, Telangana, India

P. Kara De Maeijer
Faculty of Applied Engineering, University of Antwerp, Antwerp, Belgium

B. Nematollahi
Department of Civil and Structural Engineering, The University of Sheffield, Sheffield, UK

K. K. Ramagiri
Department of Civil Engineering, Indian Institute of Technology Hyderabad, Sangareddy, Kandi, Hyderabad, Telangana, India

L. Rossi · F. Dehn
Institute for Concrete Structures and Building Materials (IMB), Karlsruhe Institute of Technology (KIT), Karlsruhe, Germany

S. Zhang · G. Ye
Section Materials and Environment, Department of 3Md, Faculty of Civil Engineering and Geosciences, Delft University of Technology, Delft, The Netherlands

M. Zhang
Department of Civil, Environmental and Geomatic Engineering, University College London, London, UK



G. Ye and F. Dehn (eds.), *Mechanical Properties of Alkali-Activated Materials*, RILEM State-of-the-Art Reports 46, https://doi.org/10.1007/978-3-032-07116-3_9

characteristics depending on the intended usage of concrete. The present chapter reviews the different types, orientations, dosages, and geometric properties of fibers included in AAC. along with the effects of fiber addition on the mix design, mixing and curing procedure of concrete, as well as the fresh and hardened characteristics of fiber-reinforced alkali-activated concrete (FRAAC). The use of statistical models to predict the mechanical characteristics of FRAAC is also discussed. Finally, the chapter presents the advantages, disadvantages, and safety precautions for this material followed by recommendations for practical usage.

**Keywords** Alkali-activated concrete · Fiber reinforcement · Fresh properties · Mechanical properties

## 1 Introduction

Global annual cement consumption is estimated to be 4.42 billion tonnes in 2021, with a steady annual growth rate of 2.96% through 2018–2021, and a further 10% increase by the end of the decade [1]. Several alternative binders are explored to reduce the associated $CO_2$ emissions and natural limestone depletion. Cradle-to-gate life cycle assessments (LCAs) show that the usage of AAC can reduce energy consumption by approximately 40%, greenhouse gas emissions by around 70%, water demand by 25%, and other environmental toxicity impact factors by 22–94% as compared to Portland cement concrete (PCC) [2, 3]. Despite its many advantages, AAC experiences deterioration attributed to the development of microcracks induced by both drying and autogenous shrinkage. AAC is prone to cracking owing to its brittle and inelastic character associated with the matrix and aggregate bond, commonly referred to as the interfacial transition zone (ITZ) [3, 4]. Existing studies report that the inelastic nature and ductility of AAC can be enhanced through the addition of fibers. The performance of fiber-reinforced AAC (FRAAC) is largely determined by the intrinsic characteristics of the fiber, interfacial bonding and fiber content, in addition to the curing conditions, mechanical properties of the matrix, and age as in the case of plain AAC [5]. Hence, the present chapter discusses the important aspects of FRAAC, starting with the definition of FRAAC, followed by the classification of fibers and the effects of fiber geometry and dosage on the workability and mechanical strengths of AAC. Additionally, the chapter reviews the previously reported statistical analysis of the mechanical properties of FRAACs. Finally, the chapter concludes by outlining the merits and demerits of FRAAC along with its potential application in the construction sector.

## *1.1 Definition of FRAAC*

PCC is generally considered to be a composite material consisting of coarse aggregates, fine aggregates, and a binder that hydrates to form a hardened matrix. AACs are generally composed of precursors that are rich in aluminosilicates and an alkaline solution that reacts to produce a hardened matrix resembling the conventional hydrated cementitious paste [1, 3, 4]. As in the case of conventional PCC, AACs are also weak in tension. The observed splitting tensile strength of ambient-cured fly ash based AAC only amounts to 2–3 MPa after 7 days, and the flexural strength is barely 0.63 MPa after 28 days, rendering the material susceptible to cracking. The microcracks triggered by the application of load, further advances to macrocracks, deterioration, and failure, rendering the material incapable of withstanding additional stress [6]. To address the issue of low early strength, one possible approach is to replace the fly ash precursor partially or fully with slag. Another option is to reinforce the AACs with fibers to produce fiber-reinforced AAC (or FRAAC) and improve the ductility, toughness, and crack resistance of the composite. One of the possible solutions to overcome this issue is the addition of fibers. Fiber-reinforced concrete (FRC) has discrete, evenly spaced-out, yet randomly distributed fibers incorporated in its cementitious matrix. By bridging the microcracks, the fibers relieve the strain accumulated in the matrix, thus preventing the formation of a continuous network of cracks. Stress transfer between the matrix and fibers is established via their interfacial bond [7]. It should be emphasized, however, that the performance of fiber-reinforced concrete are dependent on several parameters, including the concrete matrix properties and the material, size, form, and elastic modulus of the fibers [8]. Detailed information about these characteristics of commercially available fibers are presented in the following sections of this chapter. Based on the findings from existing studies, FRAACs appear promising for use in construction through attempts to enhance durability and service life while lowering the repair and maintenance costs compared to conventional concrete. However, a detailed environmental impact analysis of FRAACs is still needed to determine whether they are a more sustainable alternative to conventional concrete [9].

One of the principal requirements for structural concrete is the mechanical resistance to applied loading during the service life. The essential indicators of load bearing capacity of concrete are allowable peak stress and toughness. Generally, microfibers (typically > 40 mm) are known to resist the crack propagation, while microfibers (typically < 40 mm) produce a pullout effect in concrete, resulting in a higher peak load. The length and diameter of the fibers come into play when a crack is isolated and develops into a macrocrack, allowing stress bridging across cracks to limit their growth [10]. Pull out and crack bridging (Fig. 1) are two main processes that control the propagation of fractures, resulting in enhanced mechanical strength and toughness in FRAAC [11].

The fibers used as reinforcement in FRAAC can be in various forms such as threads, filaments, whiskers, and nanofibers. The three principal criteria governing the selection of fibers as reinforcement in traditional concrete as well as in FRAAC

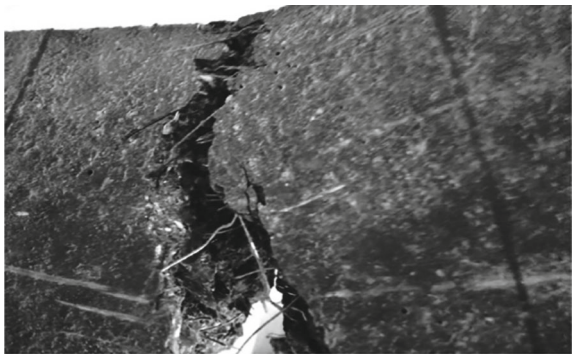

**Fig. 1** Pulling out of steel fibers in FRAAC exposed to flexural loading [11]

are: (1) compatibility of fiber characteristics with the desired applications such as shrinkage reduction, improvement of post-cracking performance, high ductility and impact resistance, (2) adequate bonding between the matrix and the fiber to facilitate the transmission of stresses, and (3) optimal geometry of the fiber for effective post-cracking performance. Before discussing the composite action of fiber and hardened alkali-activated matrix, it is important to classify the fibers commonly used as reinforcement in concrete, based on material and geometric properties. The various types of available fibers are broadly categorized in this section based on their geometry and type, with more specific classifications as indicated in the flowchart that follows (Fig. 2).

## *1.2 Fiber Classifications*

### Synthetic Fibers

*Steel fibers*

Steel fibers possess high mechanical strength, flexibility, and availability, resulting in their popularity as reinforcement for cementitious systems. Based on usage, they can be classified as (1) pieces of smooth or deformed cold-drawn wire, (2) smooth or deformed cut sheet, (3) melt-extracted, (4) mill cut, and (5) modified cold-drawn wire steel fibers that can be dispersed in concrete [15]. These fibers exhibit a tensile strength of about 310–2850 MPa and ultimate elongations of 0.5–3.5%, based on the material type and fabrication process [14]. Steel fibers possess a corrugated surface, leading to enhanced fiber-matrix interlocking due to the manufacturing processes and malleability of the source material [16, 17]. However, the main problem with steel fibers is the tendency of corrosion [18, 19]. As a result, the fibers are used in the form of stainless steel alloys [20], or coated with composites such as copper/zinc [21, 22] in PCC to reduce the possibility of corrosion.

There are several studies reported on the impact of steel fiber addition on the performance of AAC [4, 6, 8, 9, 11, 23–27]. In all cases, as for steel fiber-reinforced

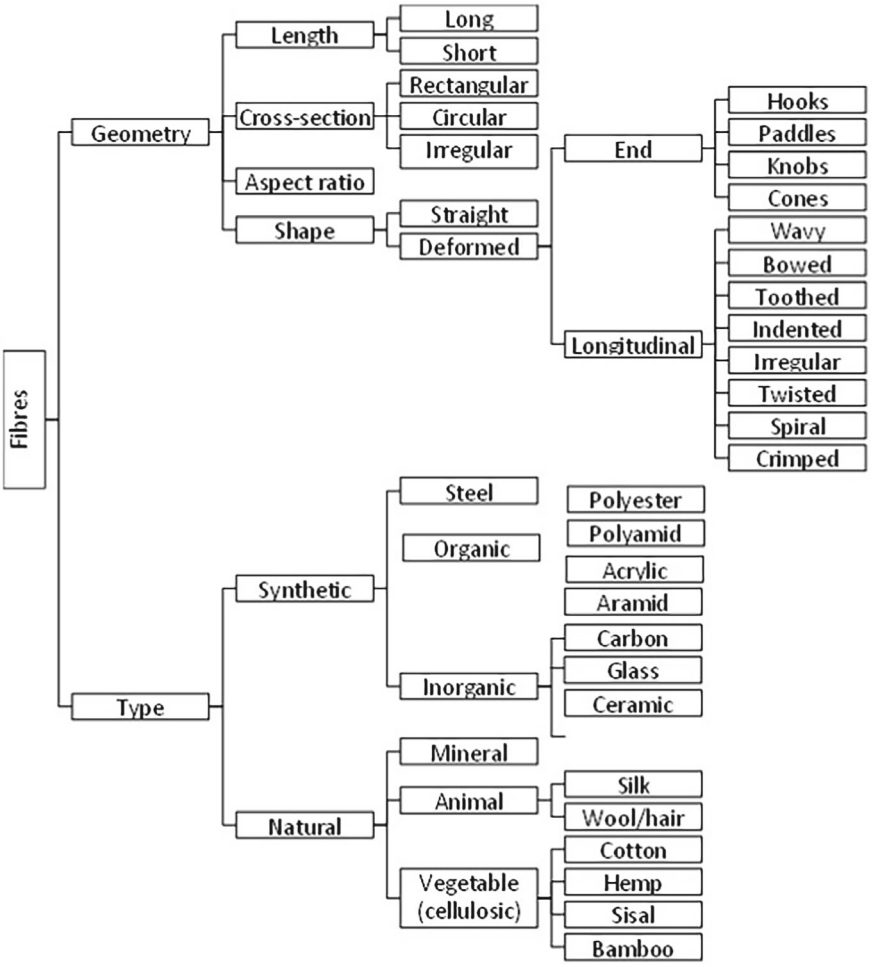


**Fig. 2** Classification of fibers used in concrete [12–14]

PCC (FRPCC), the workability of FRAAC is compromised upon the addition of steel fibers. However, this reduction in workability is observed to be less prominent for steel fibers compared to other types of fibers such as waste steel wool, PVA, PP, carbon, and polyester [23]. Despite the reduction in workability, the addition of steel fibers leads to various advantages. The bond between the fiber and the AAC matrix was found to be enhanced due to the continuous polymerization of the binder, which reduced the drying shrinkage to as low as 400 microstrains (με) [6, 24]. Steel fibers exhibit a higher elastic modulus and greater tensile strength compared to synthetic and natural fibers [10]. For fly ash-slag blended and slag based AACs, the incorporation of steel fibers resulted in 9 and 26% greater ultimate tensile strength compared to the inclusion of polyethylene fibers [26]. Owing to the aforementioned reduction in

workability caused by the addition of micro-steel fibers, there is usually a limit of 2% by volume on their inclusion in concrete. The recommended dosage for macro fibers is not more than 1% because of the drastic reduction in workability. Additionally, the specific gravity of steel fibers is 7850 kg/m$^3$ and their manufacturing process is energy intensive. Hence, relatively less expensive and lightweight alternatives are being explored, as discussed below.

*Organic Fibers*

Another type of fibers used for reinforcing cementitious systems are hydrocarbon-based polymeric fibers. Polymers are fundamentally long chains of monomer units, bonded through strong intermolecular forces [28]. The intermolecular interaction varies for different polymers and changes their properties. Depending on the order of chains, polymers are also classified as crystalline (over 80% crystallinity), semi-crystalline (10% < crystallinity < 80%), and amorphous (less than 10% crystallinity) polymers [29, 30]. Increasing the crystallinity of polymers can enhance mechanical properties, elastic modulus, environmental stability, and surface roughness. Furthermore, polymeric fibers can be categorized into synthetic and natural fibers based on their source materials and production process.

A popular subcategory of polymeric fibers are synthetic polymer fibers. These are extensively produced from raw materials or recycled from plastic wastes. The usage of recycled fibers in construction is a formidable solution for disposal of the widely consumed plastics such as polyethylene terephthalate (PET) and polypropylene (PP) [28]. The most used synthetic fibers in cementitious matrixes are based on PP, polyvinyl alcohol (PVA), polyethylene (PE), and PET. PP is derived from the monomer $C_3H_6$ and is a pure hydrocarbon like paraffin wax in a variety of shapes and sizes, and with differing properties such as tensile strength, elongation, elastic modulus and so on [31]. The main advantages of these fibers are inexpensive cost, inert characteristics at high pH of the cementitious environment, controlling plastic shrinkage cracking of the concrete, and easy dispersion [32]. However, it suffers from poor thermal resistance, low modulus of elasticity (MoE), and poor interfacial contact with cementitious matrices due to its inherent hydrophobic characteristics [33–36]. Recently, the recycling of PET bottles to produce fibers have shown a promising future for construction applications. PET fibers have comparable mechanical properties with PP and nylon fibers, while their production is more cost-effective and environmentally friendly [37]. The PVA fiber, on the other hand, has higher tensile strength of ~0.8–2.5 GPa and a MoE of 29–42 GPa. Moreover, it has a strong chemical bonding with cementitious and both fly ash and slag-based alkali-activated binders due to the presence of the hydroxyl group in its molecular chains [38–41]. However, PVA fibers are relatively expensive [41] and the high chemical bonding of these fibers leads to a tendency of fiber rupture, and thus limits the tensile strain capacity of the composite [38, 42, 43]. The properties of PE fibers are significantly dependent on their molecular mass, polydispersity, and degree of crystallinity [44]. The tensile strength and elastic modulus of a high-density PE fiber can be as high as around 3.5 GPa and 110 GPa, respectively [43]. This material also has hydrophobic characteristics [45, 46].

*Inorganic Fibers*

Among the inorganic fibers, glass and carbon fibers are regarded as the most widely used fibers across the globe. Inorganic fibers containing alumina and silica have also been reported in the literature [47]. In addition to low cost, high tensile strength, and chemical stability, these fibers exhibit high melting points and are suitable for high-temperature applications such as refractories due to their excellent insulating properties [48]. Inorganic fibers are produced using different techniques based on the source material. These techniques include rod drawing to produce wires; passage through an orifice to produce melt-spun fibers; vapor-plating boron on a tungsten core; crystal growth from a melt solution or by the vapor-liquid-solid technique for synthesizing whiskers; and chemical reactions to produce silicon carbide (SiC) fibers by the pyrolysis of polycarbosilane based fibers [47, 48].

One of the commonly used ceramic inorganic fibers are silica fibers having a high content of pure $SiO_2$. These fibers are commercially available as E-glass (electrical glass), S-glass (structural glass), C-glass (chemical glass), and AR-glass (alkali-resistant glass). AR-glass fibers are specifically aimed at reducing the degradation of glass fibers in highly alkaline environments [34, 49, 50]. Another type of inorganic metal oxide-based fiber is aluminosilicate fiber. This fiber is composed of 45–60% $Al_2O_3$ and the remaining content is made up of silicates. It is reported that fibers containing about 52% $Al_2O_3$ can resist 1250 °C and even higher temperatures. The tensile strength of these fibers is directly proportional to the silica content and inversely proportional to their elastic modulus [47]. Furthermore, basalt fiber, which is derived from volcanic rocks, is produced through a melting process at the temperature of about 1500–1700 °C [51]. Basalt is an easily available, inexpensive, and non-reactive fiber. It exhibits desirable tensile strength, durability, and thermal characteristics. It has a hardness of around 8–9 on the Moh's hardness scale, resulting in excellent abrasion resistance [52]. Additionally, it exhibits adequate resistance to acid attack [53]. Basalt fibers can sustain temperatures from about 200 up to 700–800 °C, although structural changes are observed at higher temperatures [54].

Carbon fibers (CF), on the other hand, have a wide range of applications and currently has a fairly large market [55]. CF have the lowest density and the highest tensile strength amongst fibers used for reinforcement. These fibers also possess outstanding mechanical, thermal, chemical, and electrical conductivity characteristics [56]. These fibers undergo negligible fatigue deformation under cyclic loading [57, 58]. Based on their elastic properties, the modulus of elasticity of CF can be classified as low (less than 200 GPa), standard (~230 GPa), intermediate (~300 GPa), high (more than 350 GPa), and ultra-high (more than 600 GPa). Based on geometry, carbon fibers can be classified as continuous fibers and carbon nanofibers [59]. Another popular type of carbon-based fibers is polymeric CF. These fibers are mainly derived from carbon-rich materials like polyacrylonitrile (PAN), petroleum pitch, and rayon [60]. Out of these, around nine-tenths of commercially used fibers are PAN based owing to their optimal tensile strength and production cost [61]. CF exhibits tensile strength in the range of 2.5–7 GPa and tensile modulus of 250–400 GPa with a low breaking elongation of only 0.6–2.5% [60]. Pitch fiber is a residue of

the oil refining industry. It shows a superior tensile modulus of up to 900 GPa with a lower tensile strength of ~1.5 to 3.5 GPa in comparison with PAN-based fibers [62]. Rayon-based fibers are less favorable due to the lower modulus of 35–60 GPa and are mainly used in carbon–carbon applications where low thermal conductivity is favored [63].

On the other end of the spectrum, carbon nanofibers are produced as whiskers, with diameters not greater than 0.5–1.5 μm. The performance of CF is mainly determined by the structure of graphite crystallites in their microstructures [59]. These fibers are commonly used in the form of carbon nanotubes (CNTs) and consist of rolled-up graphene sheets made of over 1000 high-aspect-ratio tubes [64]. They are synthesized in single-wall CNTs and multiwall CNTs with a tensile strength of 11–63 GPa and extremely high Young's modulus of 1–1.8 TPa [65, 66]. Different types of graphene have been successfully produced such as graphene oxide (GO) and reduced graphene oxide. GO shows high performance and flexibility because of its highly oxidized nature, although it has large number of surface residual epoxides, hydroxyl, and carboxylic acid groups, and therefore, there is a wide range of chemically reactive groups for various functionalization purposes [29]. CNT or GO inclusion is used to produce high-performance cementitious composites with higher energy absorption as well as high electrical and thermal conductivity by incorporation of very small fiber content [67, 68]. There are some other inorganic fibers such as boron, boron carbide, boron nitride, zirconia, silicon carbide, silicon nitride, and different whiskers with high mechanical properties and thermal resistance developed for specific PCC applications [47, 48, 55]. There can be future studies on the inclusion of these fibers in FRAAC.

**Natural Fibers**

As an alternative to synthetic fibers, natural fibers are also gaining popularity to avoid extensive manufacturing processes. For the development of environmentally friendly and energy-efficient materials, monofilament cellulosic fibers such as jute, hemp, kenaf, bagasse, and sisal are regarded as alternatives to synthetic fibers in cementitious composites [69]. These fibers are widely available and have a low price, low density, reduced thermal conductivity, and acceptable mechanical properties. In contrast to synthetic fibers, that require more energy for its production, natural fibers are reproducible and are more affordable [13]. However, there are some major problems with these fibers, namely low durability, efficiency at high fiber content that reduces the workability of the fresh composite, inconsistent material properties, and poor interaction with the matrix [69–71]. Natural fibers such as luffa [72], jute, sisal, and curaua fibers [73], have also been applied in AACs. However, Wei and Meyer [74] found that the cellulose in natural fibers could easily be damaged by the high-alkali environment. Hence, the long-term durability of AACs incorporating natural fibers needs to be studied extensively before its practical implementation.

Based on the findings discussed in this section, steel, PVA, and PP are the fibers recommended for practical usage in the production of FRAAC. The next section discusses the influence of fiber geometry on the efficiency in enhancing concrete characteristics.

## *1.3 Geometry*

Fibers are produced in a wide variety of geometric forms. Based on geometry, reinforcements can be classified into fibers, whiskers and particles. Figure 3 shows that the tensile strength of the fiber decreases with an increase in its diameter, irrespective of the type of fiber. This is owing to the belief that fibers with larger diameter contain more flaws and defects than single-crystal whiskers or micro fibers [47, 48]. This effect is much more evident in fibers having greater tensile strength.

Furthermore, the fiber-binder interaction can be enhanced by pre-deforming the fibers in the production phase to provide a better mechanical anchorage. As illustrated in Fig. 4, this deformation may be applied to the fiber in a variety of ways.

Fiber cross-sections, too, exist in a number of shapes and sizes, as well as multifilament and monofilament networks that split during mixing. In addition to their cross-section, fibers are classed as solid and coated (copper and silicon carbide (SiC) coated) fibers as shown in Fig. 5.

### Fiber Diameter and Aspect Ratio

In the case of non-circular fibers, an equivalent diameter is the diameter of a circle with an area equal to the cross-sectional area of the fiber. In the case of circular fibers, the effective diameter is the minimal diameter along the length of the fiber, since it indicates the maximum load-carrying capacity.

The aspect ratio of fiber is calculated by dividing the fiber length by the corresponding fiber diameter to determine the slenderness of an individual fiber. This value ranges from 40 to 2000 for short fiber-reinforced composites, although it is usually less than 300. Summarized information pertaining to the characteristics of

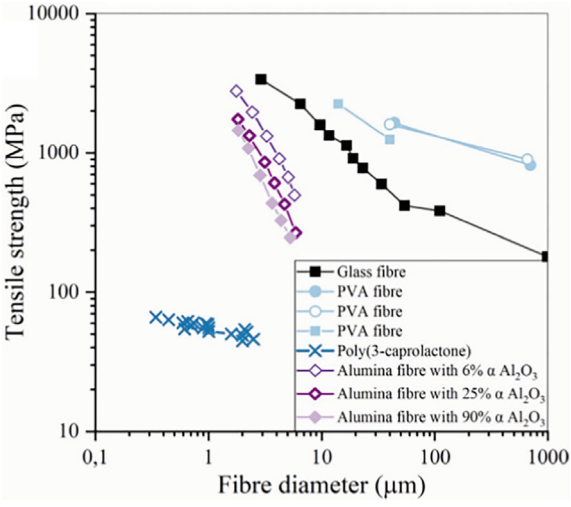


**Fig. 3** Relationship between tensile strength and fiber diameter for FRAACs with different fiber types [14]

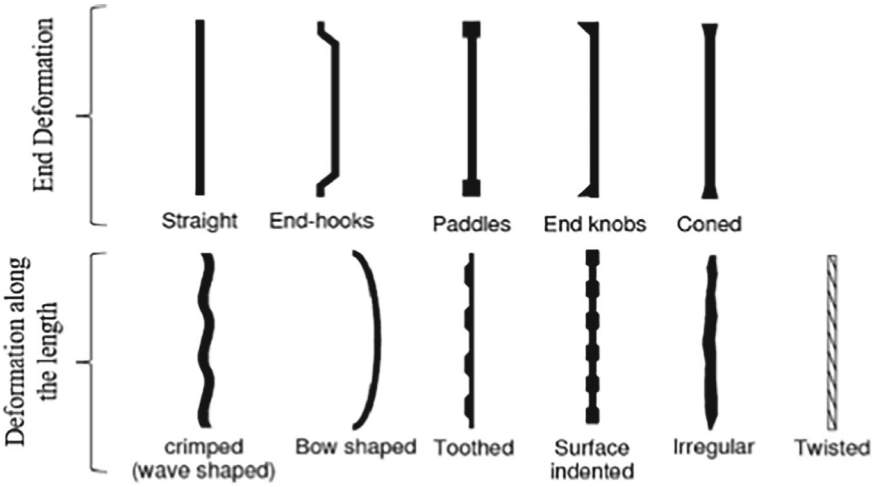


**Fig. 4** Longitudinal geometry of fibers

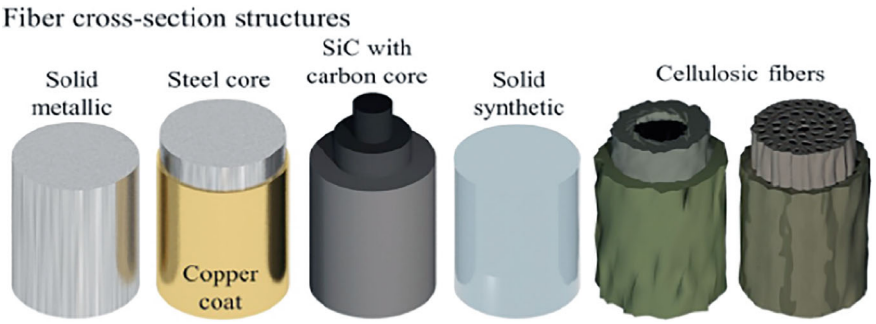


**Fig. 5** Structural cross-section of fibers [14]

different types of commercially available fibers is presented in Table 1. The information provided in Table 1 can be used to select the type of fiber based on the application.

Fiber density is usually expressed in g/cm$^3$ although the linear mass density of fibers can be measured in denier or den if the specific gravity is known. Synthetic fibers are commonly measured in this unit [75, 76]. In recent years, denier has been supplanted by a 1 g/km international unit known as "tex" [77].

### Fiber Count and Specific Surface

The quantity of fibers and their surface area impact the formation of cracks along and around the fibers. The surface area of the afflicted fibers is one of the important factors in determining the debonding in AAC, while the mechanical and bond characteristics along with the cross-sectional area of fibers within the crack plane governs pull-out.

**Table 1** Properties of commercially available fibers [14, 29, 47, 49, 60, 75]

| Types | Tensile strength (MPa) | Young's modulus (GPa) | Ultimate elongation (%) | Specific gravity | Influence on properties of the composite |
|---|---|---|---|---|---|
| Steel | 310–2850 | 20 | 0.5–3.5 | 2.50 | Enhanced mechanical strength and ductility, Reduced drying shrinkage |
| Glass | 1034–3792 | 69 | 1.5–3.5 | 3.20 | Enhanced mechanical strength, Resistance to high temperature |
| Carbon | 2500–7000 | 250–400 | 0.6–2.5 | 1.80 | Enhanced mechanical strength, Resistance to fatigue loads |
| Pitch | 1500–3500 | 50–950 | – | 1.9–2.16 | Enhanced mechanical strength |
| Rayon | 1500–2400 | 35–60 | 15–40 | 1.52 | Low thermal conductivity |
| Carbon nanotubes | 11000–63000 | 1000–1800 | – | 1.3–1.4 | High energy absorption, Enhanced mechanical strength |
| PVA | 800–2500 | 29–42 | 7 | 1.29 | Reduced plastic shrinkage, Enhanced mechanical strength, Inert at high pH, strong chemical bonding with AAB matrix |
| Polypropylene | 551–758 | 3.45 | 24 | 1.10 | Reduced plastic shrinkage, Inert at high pH |
| Nylon | 827–858 | 4.13 | 16–20 | 0.50 | Reduced plastic shrinkage, Inert at high pH |
| Cotton | 413–689 | 4.82 | 3–10 | 1.10 | Low density, Reduced thermal conductivity |
| Hemp | 270–900 | 23.5–90 | 1–3.5 | 1.4–1.5 | Low density, Reduced thermal conductivity |
| Polyethylene terephthalate | 420–450 | 3.1–10 | 11.2 | 1.3–1.5 | Reduced plastic shrinkage, Inert at high pH |

(continued)

**Table 1** (continued)

| Types | Tensile strength (MPa) | Young's modulus (GPa) | Ultimate elongation (%) | Specific gravity | Influence on properties of the composite |
|---|---|---|---|---|---|
| Polyester | 580–1100 | 15 | 35 | 1.22–1.38 | Reduced plastic shrinkage, Inert at high pH |
| Jute | 250–350 | 26–32 | 1.5–1.9 | 1.3–1.5 | Low density, reduced thermal conductivity |
| Kenaf | 223–930 | 14.5–53 | 1.5–2.7 | 1.4 | Low density, reduced thermal conductivity |
| Sisal | 280–750 | 13–26 | 3–5 | 1.34–1.45 | Low density, Reduced thermal conductivity |
| Bagasse | 222–290 | 17–27 | 1.1 | 1.3 | Low density, reduced thermal conductivity |
| Basalt | 3000–4840 | 89–110 | 3–3.15 | 2.65–2.80 | Resistance to acid attack and high temperature |
| Silicon carbide | 2200–3450 | 221–250 | – | 2.5–2.7 | – |
| Silicon nitride | 2500–4800 | 195–300 | – | – | – |
| Boron nitride | 2100 | 345 | – | 7.65–7.85 | – |

Additionally, the theory that energy will be used by fractures that pass through or around the fibers is correlated with both the quantity and surface area of the fibers that are encountered. Finally, the cross-sectional area of fibers within the crack plane, as well as the elastic properties and bond patterns of the fibers, will all influence the potential of fibers to transfer stress across a crack. As a result, the reinforcing area, fiber specific surface, and fiber count are of great relevance. These characteristics can be estimated as specified by Refs. [14, 75].

## *1.4 Fiber Content*

The cumulative effect of the complete network of fibers and their orientation with the matrix determines the overall performance of the composite. In general, increasing the fiber content leads the matrix to generate many microcracks rather than a few macrocracks, which improves the ductility of the concrete. With the incorporation of hooked-end steel fibers, concrete exhibits a tensile/flexural softening behaviour or, in some cases, a mild post-hardening behaviour when the initial crack load exceeds, and the residual load reduces with increasing deformation [78].

The compressive strength of the composites increases with increasing fiber dosage up to a certain optimal value, regardless of the type of fiber, which is attributed to the

homogeneous matrix that may be achieved with a lower fiber dosage. However, up to 1% fiber volume fraction, the inclusion of hooked end steel fibers in AAC has no significant impact on the compressive strength [79]. Furthermore, in the fresh stage, inadequate compaction of the composite with high fiber content results in a highly porous structure with heterogeneous fiber-matrix interaction. The improvement in compressive strength with an increase in fiber dosage is less significant as compared to the corresponding increase in flexural strength. However, the enhancement in post-cracking residual flexural strength and ductility outweighs the rise in flexural strength [79]. Increased fiber dosage enhances the bridging effect, which results in the generation of many microcracks rather than a few macrocracks, which is a major factor in the development of flexural strength [80]. Cracks usually initiate at the weakest region in the fiber-reinforced matrix. Normally, this relates to the fiber/matrix interface and other flaws in the matrix such as pores and air bubbles. In these regions, the applied stress can easily exceed the tensile strength of the matrix. The fibers provide a bridging effect in this case, transferring stresses within the composite matrix. In the presence of a conducive curing regime, this continuous bridging effect and transfer of stresses lead to the development of many microcracks and pseudo strain hardening under tensile loading condition [40, 43, 81]. The matrix strength and fiber-binder interaction, on the other hand, evolve with time, resulting in an enhanced load-bearing capacity of the composite [82].

Despite all the information available on FRAAC, there are no reported standard codes of practice for the practical use of these materials. Hence, this study contributes to existing knowledge through the following discussion on mix proportions, mixing and curing procedure, mechanical characteristics, and the potential for practical applications of FRAAC.

## 2 Mix Proportions, Mixing and Curing Procedure for FRAAC

### *2.1 General Approaches to Designing of Mix Proportions*

Traditional cement-based concrete mix proportions are generally selected based on the requirements of the target density, mechanical strength, and workability. In comparison to AAC without fibers, the key demands for FRAAC are improved tensile and flexural strength, fire resistance, and/or shrinkage mitigation. It is reported in several studies that a binder content of around 450 kg/m$^3$ is recommended for AAC [78, 83]. The target density is around 2400–2500 kg/m$^3$ [83, 84]. The workability, measured in terms of slump, is desired to be in the range of S2–S4 as per BS EN 8500-1:2015 [85] to encourage the practical application of FRAAC. The fiber content in FRAAC reportedly ranges between 0 and 0.6% by volume of concrete (different guidelines apply for engineered cement composites), irrespective of the fiber type [14, 78]. However, the addition of most fibers beyond 0.3% by volume of concrete

leads to a decrease in workability due to the clumping of fibers. This effect is more prominent for PVA fibers compared to steel fibers. Hence, it can be recommended to use the dosage of fibers by volume of concrete depending on the purpose and requirements of mechanical and flow properties of the FRAAC.

### *2.2 General Approaches for Mixing and Curing of FRAAC*

Previous research studies have adopted different mixing and curing techniques for the production of FRAACs. The most commonly used alkaline activator is a combination of solid NaOH, sodium silicate (or waterglass) and water at the required proportions. It is a general practice to prepare this mixture 24 h before the blending of concrete in order to attain the required homogeneity. Prior to adding sodium silicate, the determined amount of NaOH and half of the water required for producing FRAAC are combined and allowed to cool until they reach room temperature [84, 86]. To produce the FRAAC mixture, all the dry raw materials such as coarse aggregates, fine aggregates and the precursors are mixed thoroughly for about a minute in the mixer. Subsequently, the activating solution is added to the mixer with a mixing time of 30 s, and then the additional water required is added. The total mixing time is recommended to be 3–5 min until a workable and homogeneous mass is obtained. It is customary to incorporate fibers either before or after the addition of alkaline activator. However, the fibers are to be added gradually using a guided strainer to ensure uniform blend with the AAC. As soon as the FRAAC mix is ready, slump test should be performed immediately. The FRAAC mix is recommended to have a slump as mentioned in the previous section. Before filling the FRAAC mix in the formwork, it is recommended to use vibro-table (approx. 30 s) to ensure better compaction of the concrete mix. After filling the formwork, the member prepared with FRAAC is recommended to be covered with a plastic sheet to prevent the loss of moisture to the atmosphere in case of sealed curing. Other types of curing can be adopted depending on the strength requirements. The next section discusses the fresh and hardened characteristics of FRAAC.

## 3 Fresh and Hardened Mechanical Properties of FRAAC

The mechanical behaviour of fresh and hardened alkali-activated concrete incorporating fiber reinforcement cannot be easily generalized, as it is directly dependent on the characteristic of the matrix (binder and activator types, mix design proportions, compressive strength), fibers (material, geometry, aspect ratio, dosage) and their interaction. The following section gives basic assumptions which can be generally observed in FRAAC, regardless of the matrix and fiber types. However, due to the amount of parameters affecting the performance of FRAAC, minimal variations in

the material composition, i.e. different binder, activator or fiber dosage, can lead to a different mechanical response of the composite.

## *3.1 Fresh Properties*

*Workability of FRAAC Mix*

As for plain concrete, the fresh properties of FRAAC are commonly determined by evaluating its workability, which is given by the setting time, density, air content and consistency of the composite. The workability can be evaluated by performing the standardized tests developed for traditional cement-based concrete, such as the slump test, flow test and Vee bee consistometer test. The workability of FRAAC, as for FRPCC, is mainly dependent on the fiber reinforcing index ($RI_v = (l_f/d_f) \cdot v_f$; where $v_f$ is the fiber volume, $l_f$ is the fiber length, $d_f$ is the fiber diameter), in addition to fiber material. In general terms, when added in low volume fractions, short fibers with a low aspect ratio have a limited effect on the workability of concrete, while the use of higher volume fractions or the use of longer fibers with higher aspect ratio can have a more significant effect on the fresh properties of the composite [87]. Thus, it is fundamental to evaluate the fiber dispersion and distribution in the mixture, avoiding segregation and fiber clustering or balling, as shown in Fig. 6.

Depending on the application of composite, the fresh properties of FRAAC can vary significantly. However, they should satisfy the same requirements defined for traditional PCC reinforced with the same fiber type and dosage. Although the workability of the composite generally decreases with the increase of the fiber dosage [89], regardless of fiber material and geometry, it is not possible to define a common threshold value for every fiber type used in construction. The fiber type, geometry, and dosage need to be defined according to the application and the required mechanical performance.


**Fig. 6** Clumping of fibers in FRAAC [88]

*Effect of Chemical Admixtures in FRAAC*

The use of superplasticizers (SP) or high range water reducing admixtures to increase workability is a popular technique for traditional PCC. Studies on the use of SP to improve workability without reducing the mechanical strength have been reported for AAC as well. However, there is limited information reported on the effect of polycarboxylate ether (PCE) based SP on the chemistry of AAC. Commercially available PCE-based SP are available as solutions containing water. It is not reported conclusively whether the addition of SP to AAC leads to a chemical reaction or if the SP only acts as a catalyst to facilitate the transport of the liquid activator to the unreacted residue of the solid precursor. It is also not clearly reported whether the SP get attached to the fibers like they do for cement particles in Portland cement-based systems. Additionally, it is demonstrated that the use of fibers to produce FRAAC not only reduces the workability but also reduces the setting time. For traditional concrete, retarders are used to overcome this issue. These retarders are generally salts of weak bases and strong acids ($CaCl_2$) or strong bases and weak acids ($K_2CO_3$), used in concentrations of 0.1–0.3% by mass of the binder in Portland cement-based systems [90]. However, investigations on the effect of retarders to aid in increasing the setting time of FRAAC are yet to be reported. Hence, this chapter recommends against using chemicals such as SP or retarders for FRAAC. The water content, and target strength of the FRAAC mixes can be decided accordingly.

## *3.2 Hardened Properties*

*Compressive Behaviour*

Although the primary use of FRAAC is in applications requiring high flexural and tensile behaviour, it is fundamental to also evaluate the corresponding strength of the composite under compression. The same factors affecting the fresh properties of FRAAC, as already described in Sect. 3.1, have a great influence also on the mechanical performance of the hardened concrete, in particular on the compressive response under uniaxial compression. In addition to the type of matrix, type of fiber, dosage, and their interaction with the matrix, the distribution of microcracks, the connectivity of pores and the boundary conditions of the test performed (Fig. 7) can also affect the compressive strength of the composite, as reported in previous studies [14]. However, the incorporation of fibers plays a major role in the development of mechanical strength of the composite [80], as fibers can increase or decrease the compressive strength of the plain matrix, depending on their material, geometry, dosage, distribution and orientation. Fibers aligned perpendicular to the crack opening provides a positive effect on the compressive strength of the composite, while fibers aligned in the direction of the load, act like voids, resulting in a negative effect on the compressive strength [91].

The fiber material and dosage, couple with the fiber geometry and orientation, also play a fundamental role in governing the compressive behaviour of FRAAC.

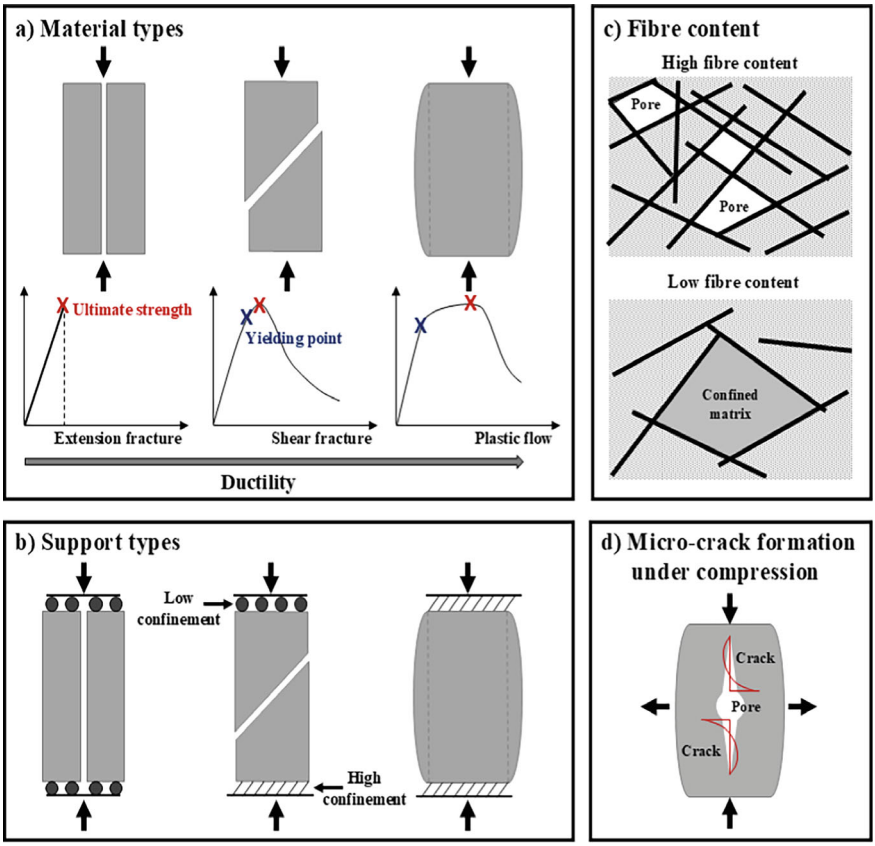


**Fig. 7** Factors affecting the compressive strength of FRAAC. Modified from [14]

As shown in Fig. 8, there is no clear correlation between the relative compressive strength, i.e. the variation of strength in comparison to the reference plain concrete, and fiber dosage, as the fiber material and geometry also need to be considered. Steel fibers generally improve the compressive strength of the composite even at fiber volume fractions higher than 2% (Fig. 8b), while polymeric and natural fibers (Fig. 8c and f, respectively) generally have a limited or negative effect on the enhancement of the matrix compressive strength, regardless of the fiber dosage. The lower MoE of these fibers reduces the crack bridging ability of the fibers, resulting in limited effects on the compressive strength of the composite.

The effect of the incorporation of different fiber types at the same volume fractions in different concrete matrices has been investigated by Köenig et al. [78]. Steel fibers and macro-PP fibers were added to alkali-activated fly ash (AAFA/AAFAA) and slag-based (AAS) concretes at 0.3% and 0.6% fiber volume fractions. Figure 9 shows the 28-day normalized compressive strength of both mixtures. All mixes incorporating

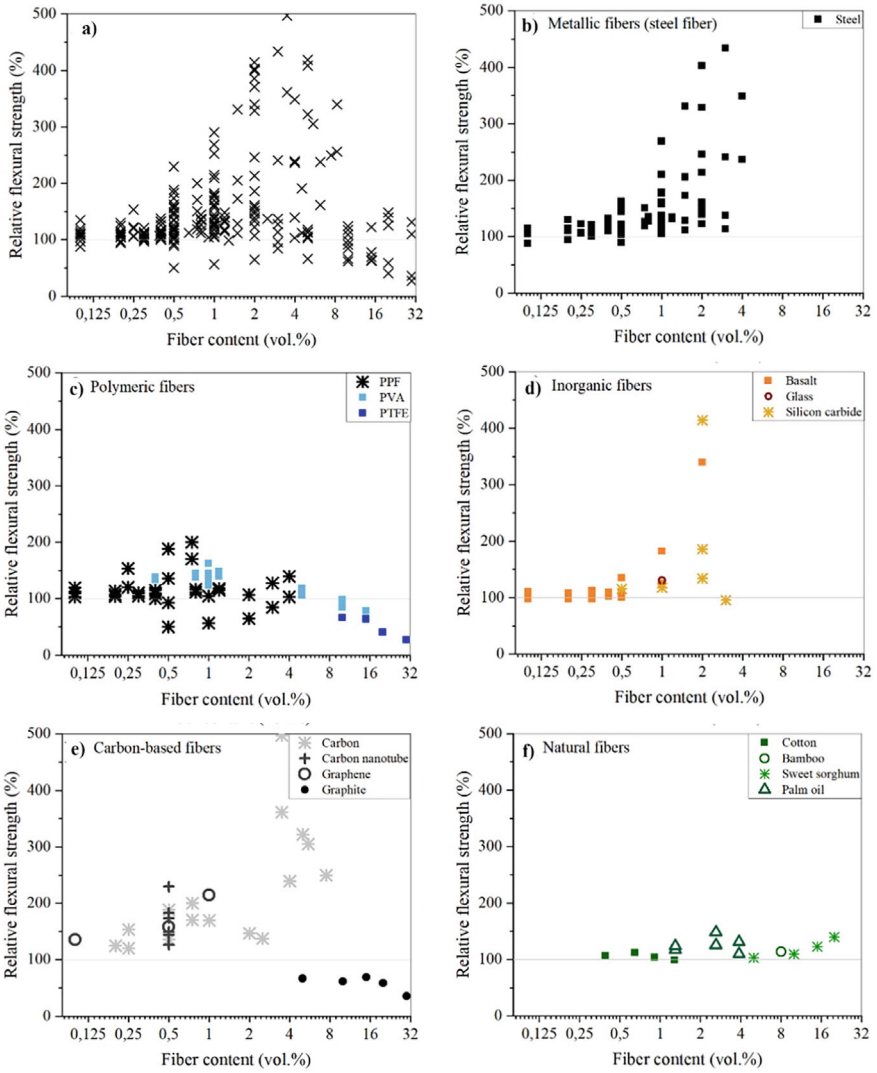


**Fig. 8** Variation of relative compressive strength in AAC reinforced with different fiber types in different volume fractions [14]

fibers, regardless of the fiber type, exhibit a reduction in strength when compared to the reference plain concrete.

The reduction in compressive strength of around 13% for AAFA/AAFAA can be attributed to the viscosity of the fresh mix and to the increased porosity due to fiber addition, resulting in a lower degree of compaction [92, 93]. The increase in fiber volume fraction from 0.3 to 0.6% increases the total porosity of the composite, especially for binder systems composed of low water and high binder contents.

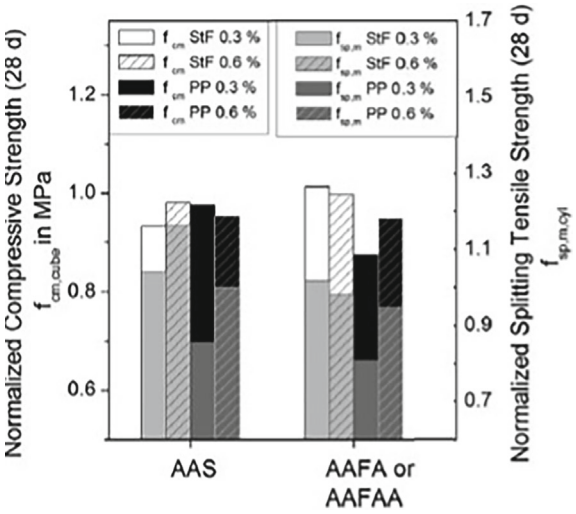


**Fig. 9** Comparison of compressive strength of FRAAC prepared with different precursors [78]

These observations are consistent for two different types of alkali-activated fly ash, namely AAFA and AAFAA reported by [78]. The study clearly demonstrates how similar fiber type and dosage can lead to different mechanical performance when added to different alkali-activated matrices. Thus, it is not possible to generalize the behaviour of FRAAC, but different matrix reinforced with different fiber types need to be evaluated separately, taking into account the characteristics of the matrix, the fibers and their interaction.

*Modulus of elasticity*

The incorporation of fibers, regardless of the type and dosage, have a limited effect on the MoE of FRAAC, as it is mainly dependent on the coarse aggregates type and volume fraction in concrete [94]. For traditional fiber-reinforced cement-based concrete with coarse-to-fine aggregate ratio (C/S) > 1, the MoE is slightly affected by the fibers in comparison to the reference unreinforced concrete. When the C/S < 1, fibers have a negative effect on the MoE, which decreases with the increase of fiber volume fraction and aspect ratio [94]. The reduction of workability due to the incorporation of fibers and their orientation with respect to the loading direction are the main causes of reduction in the MoE of FRAAC in comparison to its corresponding reference concrete. Thus, in addition to the matrix composition and aggregates type and ratio, the fiber type, shape and dosage also play a fundamental role in the MoE of FRAAC. However, the MoE of AAC with and without fibers is directly linked to the compressive strength of the composite [12]. Farhan et al. [12] evaluated the correlation between compressive strength and MoE of AAC reinforced with different fiber types and dosages (Fig. 10).

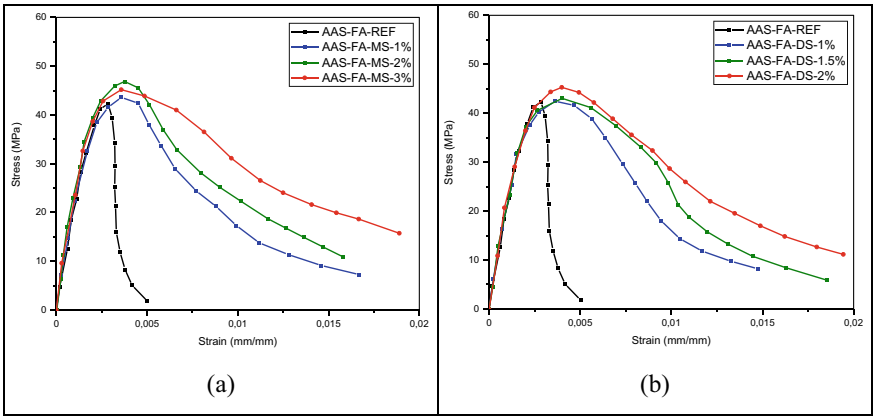


**Fig. 10** Compressive stress–strain response of ambient cured alkali-activated slag-fly ash concrete reinforced with **a** micro steel fibers and **b** deformed steel fibers. Modified from [10]

The current international standards overestimate the MoE of fiber-reinforced low-calcium alkali-activated concrete. These alkali-activated systems generally show lower MoE in comparison to OPC with similar compressive strength [95]. However, the effect of fibers on the MoE of AAC cannot be generalized as it mainly depends on the matrix mix design and on the fiber type, aspect ratio, orientation and dosage. Further experimental and analytical investigations need to be performed to better evaluate the effect of fibers on the MoE of AAC obtained with different binders and activator types and to be able to correlate the MoE with the compressive strength of the composite.

*Stress–strain response under uniaxial compression*

Fibers not only have a direct effect on the compressive strength of the composite but also affect the stress–strain response under uniaxial compression, enhancing the material post-peak behaviour, as shown in Fig. 10.

Although the incorporation of steel fibers, regardless of the fiber geometry, has a minimal effect on the ascending branch of the stress–strain curve, it has a significant impact on the post-peak descending branch. The ascending branch of the curve up to the peak stress is mainly affected by the matrix compressive strength and MoE, on which fibers have a limited effect, regardless of the fiber shape and dosage. However, in comparison to the reference unreinforced mix, the mixes incorporating steel fibers exhibit an increase of compressive peak stress and corresponding strain with the increase of the fiber volume fraction, resulting in an overall increased ductility of the composites. Once the peak stress is reached, the crack bridging effect of the fibers enhances the post-peak behaviour, resulting in less steeper curves compared to the reference mix. Owing to the incorporation of steel fibers, the material undergoes higher deformations under uniaxial compression, increasing its load-bearing capacity and overall performance.

Evaluating the stress–strain response under uniaxial compression is fundamental to derive constitutive models and design regulations for fiber-reinforced AAC, facilitating its utilization in the construction industry. Despite several analytical models developed for cement concrete reinforced with steel fibers [96], models describing the behaviour of AAC reinforced with steel or alternative fibers are still limited [97].

*Tensile behaviour*

The tensile behaviour of fiber-reinforced concrete, regardless of the matrix type, is directly affected by the mechanical performance of the matrix, the fiber material, geometry and dosage, and their interaction. Under direct tensile loading, fibers have a limited effect on the pre-cracking tensile strength of the composite, as it is mainly governed by the matrix characteristics. Once the maximum uniaxial direct tensile stress is reached, the concrete matrix starts cracking and the fibers get activated. Thus, the post-cracking behaviour of the composite is the result of the fiber-matrix interaction, as shown in Fig. 11.

The contribution of the fibers to the tensile post-peak behaviour depends mainly on the effective area of the fibers in the direction of the load and the elastic modulus of the fibers. High fiber dosages result in higher fiber effective area, leading to greater post-cracking residual strength [87]. For normal-strength concrete reinforced with low to medium fiber dosages, the tensile response of the composite is characterized by strain-softening, while at higher volume fractions, the composite exhibits strain-hardening, as shown in Fig. 12 [98]

In strain-softening fiber-reinforced concrete, the post-cracking tensile strength is lower than the matrix cracking strength and only a single crack develops and propagates when the load is increased. The majority of normal-strength fiber-reinforced cement-based or alkali-activated concrete shows this post-cracking behaviour,

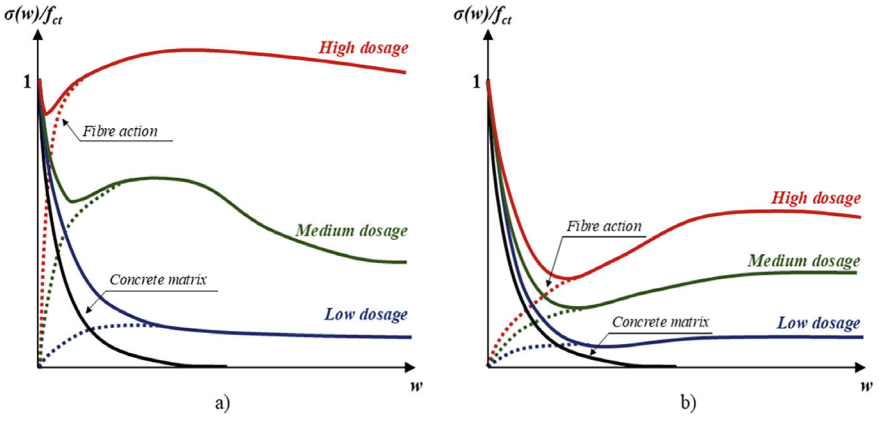


**Fig. 11** Fiber-matrix interaction in concrete with **a** fibers with a high modulus of elasticity and **b** fibers with low modulus of elasticity subjected to direct tensile load. Modified from [87]

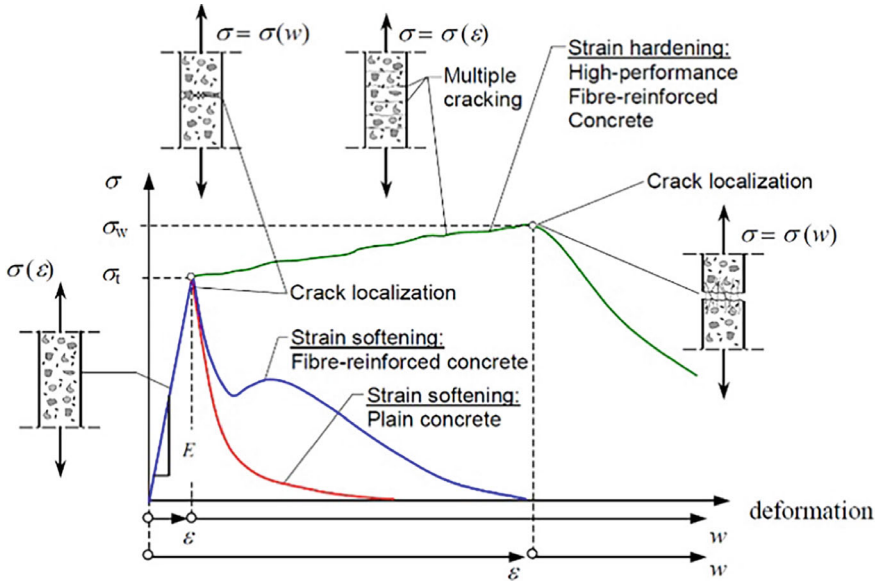


**Fig. 12** Tensile behaviour of plain and fiber-reinforced cement-based concrete [98]

although the shape of the curve is directly correlated to the fiber material, geometry and volume fraction. In strain-hardening fiber-reinforced concrete, the post-peak tensile strength is higher than the matrix cracking stress and the material shows several micro-cracks, which grow until a macro crack localizes and stresses decrease.

The tensile response of fiber-reinforced concrete, regardless of the matrix and fiber types, is usually described by a stress–strain (σ-ε) curve up to the peak tensile stress, as the material behaves elastically until the first crack localization. Once the peak stress is reached and the crack starts growing, the tensile behaviour is described by means of a stress-crack width (σ-w) curve, as shown in Fig. 12. Defining the stress–strain or stress-crack width response of fiber-reinforced concrete is fundamental to fully characterize the material behaviour and favor its design and finite element modelling.

However, evaluating the tensile behaviour of plain and fiber-reinforced concrete through direct tensile tests is still quite difficult and time consuming; in addition, the sample geometry plays a fundamental role in the fiber distribution and orientation, possibly leading to overestimations of the real tensile behaviour due to fiber alignment in the load direction. Thus, indirect tensile tests are preferred to evaluate the tensile response of the composite. The splitting tensile strength and the flexural strength tests (both 3- or 4-point bending tests) are the most commonly performed tests to evaluate indirectly the tensile behaviour of fiber-reinforced concrete and they are discussed in the following sections.

*Splitting tensile strength*

Based on available studies, it is not possible to generalize the effect of fiber dosage or fiber type on the splitting tensile strength of FRAAC. However, it is reported that the addition of fibers, regardless of the fiber material and geometry, leads to significant improvement in the composite ductility even beyond the maximum load capacity [78, 79]. The addition of steel fibers is generally reported to increase the splitting tensile strength of FRAAC using slag as the precursor [78]. This is attributed to the early fiber-activation due to bridging shrinkage-induced microcracks. However, using other types of precursors, especially fly ash, report contrasting results where the tensile strength decreases due to the addition of steel fibers. One of the possible reasons for the relatively low increase in tensile strength is the recommended limits on fiber dosage, based on the requirements of workability and compressive strength. Additionally, it is to be considered that steel fibers possess smooth surfaces that result in relatively low bond strength with the binder matrix. However, the fly ash based AAC shows higher bond with steel compared to the slag based AACs [78]. As a result, it is recommended by some researchers to use steel fibers with high stiffness and optimal cross-section as commonly found in hooked-end steel fibers. The multiple hooked-end fibers (4D and 5D) improve the mechanical anchorage resulting in a superior bond performance [79]. An advantage of these fibers is to limit the widening of microcracks [99]. It is also reported that the increase in splitting tensile strength due to steel fibers in FRAAC is higher in the case of slag-based FRAAC as compared to fly ash-based FRAAC [78]. A study on glass fiber-reinforced AAC demonstrated an optimal splitting tensile strength at 0.3% addition of 0.6 mm glass fibers, leading to a 31.6% increase in splitting tensile strength when compared to that of plain fly ash-slag blended AAC [100]. However, further increasing the fiber dosage resulted in balling of the fibers, leading to inadequate concrete compaction and the formation of voids with consequently unsatisfactory strength gain. On a contrary, the addition of polypropylene fibers at 0.5% volume fraction in fly ash-slag blended AAC resulted in a decrease of splitting tensile strength from 3.78 MPa (plain AAC) to 3.69 MPa (FRAAC). However, the addition of steel fibers at 0.5% volume fraction to the same AAC matrix resulted in an increased split tensile strength of 5.23 MPa [101].

Overall, it is reported that the increase in compressive and tensile strength is more significant for short fibers with a higher dosage. These fibers help in limiting the width of microcracks as the applied loading approaches the failure load. These fibers are also associated with a lesser reduction in the viscosity of fresh FRAAC mixes, ensuring a lower number of compaction voids.

*Flexural Strength*

The failure of a concrete specimen under loading is governed by the mode of cracking. The three possible modes are Mode I (opening), Mode II (in-plane shear), and Mode III (out-of-plane shear). AAC is reported to fail usually in Mode I due to tensile stress orthogonal to the local crack plane. The corresponding fracture stress is considerably less than those of Modes II (sliding due to shear stress parallel to the crack surface but orthogonal to the crack front) and III (tearing due to shear stress parallel to the crack

surface and the crack front) [14]. As a result, AAC specimens reportedly exhibit lower flexural strength values, especially when fly ash is used as the precursor under ambient curing conditions [86, 99]. Hence, the use of FRAAC can address these issues through greater resistance to the development and widening of cracks.

One of the critical components governing the flexural efficiency of FRAAC is the interface between the fibers and the binder matrix. Under the action of flexural load, the resulting tensile stress acts as a shearing component at this interface. The friction between the surface and the matrix and their adhesion withstands this action to prevent the development and widening of cracks. This interfacial force extends beyond the contact surface between the fiber and the matrix, and their combined action forms an annular region around the fibers [25, 80, 102]. The magnitude of this force is maximum at the interface and gradually reduces to zero with increasing distance from the interface. This mechanism resembles the action of embedded steel rebars in traditional reinforced concrete and is particularly evident in FRAAC with steel fibers [25]. On the other hand, hydrophobic fibers with smoother surfaces result in the formation of weak interfacial contact, diminishing the transfer of stress at the fiber-matrix interface [80]. As a result, the increase in flexural strength of FRAAC w.r.t. AAC without fibers is more prominent when steel fibers are used instead of PP or any other synthetic fibers. In fly ash-based FRAAC with steel fibers, nearly 13% increase in flexural tensile strength is reported [78] whereas, for slag-based FRAAC with steel fibers, an increase of 9% is reported. For slag-based FRAAC with macro-PP fibers, the increase in flexural tensile strength is reported to be as high as 22% for a fiber dosage of 0.6% by volume of concrete [78]. Another study on FRAAC with steel fibers reports that the flexural strength increases by 9.4% for fiber dosage of 0.25% by volume of concrete, and by nearly 24% for fiber dosage of 1% by volume of concrete [103]. For slag-based AAC, the addition of steel fibers greater than 1% volume fraction was reported to have a significantly high ultimate flexural strength of up to 13 MPa [104]. Additionally, the descending portion of the load-deflection curve was found to be steeper at higher ultimate strength, indicating that the residual strength decreased rapidly beyond the peak load.

The variations in compressive, splitting tensile, and flexural strength values of FRAAC are not found to follow any uniform pattern. As a result, extensive data collection is required to develop models for predicting the splitting tensile and flexural characteristics of FRAAC based on their compressive strength values. The next section discusses this in further detail.

## 4 Statistical Analysis of the Mechanical Properties

The relationships between the splitting tensile and compressive strength of plain traditional PC concrete are quite well established, as are the relationships between the flexural and compressive strength. To reduce the need for testing specimens and to save material, these relationships help in predicting the splitting tensile and flexural strength values for different grades of concrete. The predicted values aid in

identifying the suitability of these concrete specimens for different practical applications, depending on their tensile and flexural strength characteristics. However, limited studies [105] are reporting similar types of prediction models for AAC. The extent of reports for FRAAC is even less. The next section discusses the relationship between the splitting tensile strength and compressive strength of FRAAC.

## *4.1 Prediction of Splitting Tensile Strength as a Function of Compressive Strength*

One of the key components for the development of models to predict the splitting tensile strength of FRAAC is the fiber content. The predicted splitting tensile strength value is usually expressed as a function of the compressive strength and a fiber content factor. In a study on fly ash-based FRAAC with crimped steel fibers of 30 mm length and aspect ratio of 66, a prediction model for the splitting tensile strength, $f_t$, was formulated using regression analysis with the product of fiber factor, $F$, and compressive strength, $f_c$, as the independent variable as shown in Eq. 1 [103]. The fiber factor was considered as an empirical variable to include the effects of varying fiber dosages and the aspect ratio on the splitting tensile strength.

The resultant expression was in the form:

$$f_t = 0.338 \times F\sqrt{f_c} + 2.764 \tag{1}$$

For a fiber dosage varying from 0 to 1%, this model exhibited around 0.003% prediction error for a tensile strength range of 2.58–4.17 MPa. The corresponding compressive strength values were 45.37–49.23 MPa. The proposed model is based only on 28-day strength values and does not consider the effect of age on strength of FRAAC.

A study on the influence of micro-steel and micro-PP fibers on the mechanical properties of ultra-high performance slag-based AAC reports an exponential equation to express the relationship between the splitting tensile strength and the compressive strength results as shown in Eq. 2 [106].

$$\mathrm{f_t} = 4.3763 \times \mathrm{e}^{0.0041\mathrm{f_c}} \tag{2}$$

The proposed model was developed on FRAAC mixes containing 0.25% PP fibers by volume, or steel fibers ranging from 1 to 2%. The splitting tensile strength values were found to be in the range of 6.1–8.5 MPa for FRAAC with 28-day compressive strength varying from 115 to 162 MPa. The proposed model did not consider any factor to include the effect of the different types of fibers, their respective dosage, and the age of the specimen, but the $R^2$ value is reported as 0.944.

Another study on the effects of PP, steel, and composite steel-PP fibers reports a series of equations to model the static and dynamic stress–strain characteristics

[107]. This study does not directly report a relationship to predict splitting tensile strength based on compressive strength but provides an interesting approach to develop prediction models for the mechanical properties of FRAAC.

Due to the lack of available information on models to predict the splitting tensile strength of FRAAC, this study recommends extensive experimental studies to generate sufficient data for FRAAC prepared with different types and varying dosage of fibers.

## *4.2 Prediction of Flexural Strength as a Function of Compressive Strength*

As observed for splitting tensile strength, there is extremely limited information available on the development of prediction models for the flexural strength of FRAAC determined using standard four-point bending test using ASTM C78/C78M-22. It is well established that the presence of the fibers enhances the flexural characteristics of concrete. In the case of FRAAC, the dosages and types of fibers are found to have a significant effect on flexural strength. Depending on the intended purpose of the FRAAC, it is essential to have prior knowledge of flexural strength. A study on FRAAC with steel fibers [103] aims to predict the flexural strength, $f_r$, using the following expression (Eq. 3).

$$f_r = 0.218 \times \mathrm{F}\sqrt{f_c} + 5.054 \tag{3}$$

where F is the fiber factor that represents the effect of the different types of fibers and their respective dosages.

Another study using both PP and steel fibers in FRAAC adopts an exponential relationship to express the correlation between the splitting tensile strength and the flexural strength [103]. However, there is no reported expression for predicting flexural strength as a function of compressive strength. The reported model does not consider the effects of different types of fibers or their dosages. Moreover, this model does not consider the effect of age of the specimen as well, although it is reported to exhibit a regression coefficient of nearly 0.96. Due to the limited number of independent parameters and a limited number of observations, the proposed model proves to be fairly accurate. However, it is clear that there is a dearth of reported data on models to predict the different mechanical characteristics of FRAAC containing different precursors, activators, fibers, and prepared with varying fiber dosages. Owing to this lack of information on the possible mechanical performance of FRAAC, specifically in the long run, the applications of this type of material are limited and mostly restricted to the construction of precast structural elements.

The next section discusses some of the factors that can encourage the practical application of FRAAC on a larger scale and the associated disadvantages and some necessary precautions for its usage.

## 5 Potential Practical Applications of FRAAC

- Depending on the application, the fibers have a significant role in enhancing the mechanical properties of AAC. The primary objective and advantage of FRAAC is the improvement in mechanical strength, specifically the tensile and flexural characteristics through bridging effect resulting from fiber inclusions (Fig. 1).
- The improvement in mechanical properties is more prominent in the case of FRAAC with steel fiber. Additionally, the availability and cost-effectiveness of steel fibers make them a popular choice for practical usage.
- The addition of these fibers can also reduce shrinkage and enhance the post-cracking performance w.r.t. AAC without fibers [25]. The highly alkaline environment in AAC prevents the rusting of the steel fibers and increases their durability [108, 109].
- In certain applications where lightweight concrete is preferred, PVA fibers can be used despite their slightly higher cost. Their high mechanical strength, flexibility, and hydrophilic nature make them suitable for some specific applications that require strain-hardening, concrete with ultra-high ductility and impact resistance [110, 111].
- An alternative to PVA fibers is the more eco-friendly and cost-effective PP fibers in similar applications [33, 80]. Another promising field of application for PVA and PP fibers in FRAAC is 3D printing mechanism to produce reinforced structural elements, avoiding the need for framework or extensive water curing [112–114].
- Another field of application for FRAAC is in high-temperature or elevated temperature environments where carbon fibers can be used to enhance thermal resistance [115, 116]. The high strength and light weight of the carbon fibers make them ideally suited for lightweight, durable and large structures [117].
- Inorganic fibers such as basalt and silicon carbide can be used as alternatives to carbon fibers in high-temperature applications such as a tensile test setup for FRAAC at 1000 °C [118–120]. Hence, there is great potential for the widespread practical use of FRAAC with different types of fibers depending on the purpose.

## 6 Recommendations for Practical Usage of FRAACs

- For working with FRAAC, the user must always wear personal protective equipment (PPE), e.g., protective laboratory gear including lab coat with long sleeves, gloves and goggles. These protective measures have to be followed during the preparation of the activator, mixing of FRAAC and the compaction process.
- If sodium silicate/NaOH solution accidentally comes in contact with the skin of the user, immediate rinsing with water is recommended. Normally it will cause itchy skin with irritation. In case of spillage and skin contact with a higher amount of solution, not rinsing immediately will convert it into a burn.

- When blending NaOH with sodium silicate solution, it is recommended to work in a room with fresh air. It is recommended to avoid direct inhalation of the fumes resulting from the exothermic reaction between NaOH and sodium silicate solution.
- When working with steel fibers, it is recommended to wear cut-resistant gloves with inner safety lining to ensure prevention of injury from the sharp fibers.

## 7 Conclusions

This chapter presents a comprehensive review of the available literature on fiber reinforced AAC.

The fiber content in FRAAC reportedly ranges between 0 to 0.6% by volume of concrete. The fiber content depends on matrix and fiber type. PVA fibers are added up to 2% to achieve post-cracking tensile strain-hardening. Additionally, if the aggregate dimensions are reduced, greater amount of fibers can be added. However, addition of fibers beyond 0.3% by volume of concrete leads to decrease in workability due to the clumping of fibers. This effect is more prominent for PVA fibers compared to steel fibers. Hence, it can be recommended to use 0.1, 0.2, or 0.3% fibers by volume of concrete depending on the purpose and requirements of mechanical and flow properties of the FRAAC.

The increase in compressive and tensile strength is more significant for short fibers with higher dosage. These fibers help in limiting the widths of microcracks as the applied loading approaches the failure load. These fibers are also associated with lesser reduction in viscosity of fresh FRAAC mixes, ensuring lower number of compaction voids.

The variations in compressive, splitting tensile, and flexural strength values of FRAAC are not found to follow any uniform pattern. As a result, extensive data collection is required to develop models for predicting the splitting tensile and flexural characteristics of FRAAC based on their compressive strength values.

The selection of fibers is governed by the intended usage of the FRAAC. While using steel fibers, the user must adhere to the recommended safety precautions to prevent any physical injury.

With more extensive research and development of standard guidelines for practical usage, FRAAC can be implemented beyond the presently used precast structural elements and provide a viable source of sustainable construction practice.

**Acknowledgements** The authors would like to acknowledge the RILEM Technical Committee 294 Mechanical Properties of Alkali-Activated Concrete (TC 294 MPA) for providing the platform to conduct the review and obtain valuable insight on fiber-reinforced alkali-activated concrete. The authors would also like to thank their respective institutes and organizations for providing the necessary resources to prepare this chapter.

## References


1. Provis, J.L., van Deventer, J.S.J.: Geopolymers: Structures, Processing, Properties and Industrial Applications (2009)
2. Worrell, E., Price, L., Martin, N., et al.: Carbon dioxide emissions from the global cement industry. Annu. Rev. Energy Env. **26** (2001). https://doi.org/10.1146/annurev.energy.26.1.303
3. Jiang, M., Chen, X., Rajabipour, F., Hendrickson, C.T.: Comparative life cycle assessment of conventional, glass powder, and alkali-activated slag concrete and mortar. J. Infrastruct. Syst. **20** (2014). https://doi.org/10.1061/(asce)is.1943-555x.0000211
4. Hammad, N., El-Nemr, A., El-Deen Hasan, H.: The performance of fiber GGBS based alkali-activated concrete. J. Build. Eng. **42** (2021). https://doi.org/10.1016/j.jobe.2021.102464
5. Puertas, F., Amat, T., Fernández-Jiménez, A., Vázquez, T.: Mechanical and durable behaviour of alkaline cement mortars reinforced with polypropylene fibers. Cem. Concr. Res. **33** (2003). https://doi.org/10.1016/S0008-8846(03)00222-9
6. Al-mashhadani, M.M., Canpolat, O., Aygörmez, Y., et al.: Mechanical and microstructural characterization of fiber reinforced fly ash based geopolymer composites. Constr. Build. Mater. **167** (2018). https://doi.org/10.1016/j.conbuildmat.2018.02.061
7. Alomayri, T.: The microstructural and mechanical properties of geopolymer composites containing glass microfibers. Ceram. Int. **43** (2017). https://doi.org/10.1016/j.ceramint.2016.12.118
8. Ganesan, N., Abraham, R., Deepa Raj, S.: Durability characteristics of steel fiber reinforced geopolymer concrete. Constr. Build. Mater. **93** (2015). https://doi.org/10.1016/j.conbuildmat.2015.06.014
9. Abdulkareem, M., Havukainen, J., Horttanainen, M.: How environmentally sustainable are fiber reinforced alkali-activated concretes? J. Clean. Prod. **236** (2019). https://doi.org/10.1016/j.jclepro.2019.07.076
10. Farhan, N.A., Sheikh, M.N., Hadi, M.N.S.: Engineering properties of ambient cured alkali-activated fly ash-slag concrete reinforced with different types of steel fiber. J. Mater. Civ. Eng. **30** (2018). https://doi.org/10.1061/(asce)mt.1943-5533.0002333
11. Mo, K.H., Yeoh, K.H., Bashar, I.I., et al.: Shear behaviour and mechanical properties of steel fiber-reinforced cement-based and geopolymer oil palm shell lightweight aggregate concrete. Constr. Build. Mater. **148** (2017). https://doi.org/10.1016/j.conbuildmat.2017.05.017
12. Farhan, K.Z., Johari, M.A.M., Demirboğa, R.: Impact of fiber reinforcements on properties of geopolymer composites: a review. J. Build. Eng. **44**, 102628 (2021). https://doi.org/10.1016/j.jobe.2021.102628
13. Amran, M., Fediuk, R., Abdelgader, H.S., et al.: Fiber-reinforced alkali-activated concrete: a review. J. Build. Eng. **45** (2022)
14. Ranjbar, N., Zhang, M.: Fiber-reinforced geopolymer composites: a review. Cem. Concr. Compos. **107**, 103498 (2020). https://doi.org/10.1016/j.cemconcomp.2019.103498
15. ASTM A820.: Standard specification for steel fibers for fiber-reinforced concrete. ASTM (2016)
16. Yin, J., D'Haese, C., Nysten, B.: Surface electrical properties of stainless steel fibers: an AFM-based study. Appl. Surf. Sci. **330** (2015). https://doi.org/10.1016/j.apsusc.2014.12.188
17. Wang, X.H., Jacobsen, S., He, J.Y., et al.: Application of nanoindentation testing to study of the interfacial transition zone in steel fiber reinforced mortar. Cem. Concr. Res. **39** (2009). https://doi.org/10.1016/j.cemconres.2009.05.002
18. Granju, J.L., Balouch, S.U.: Corrosion of steel fiber reinforced concrete from the cracks. Cem. Concr. Res. **35** (2005). https://doi.org/10.1016/j.cemconres.2004.06.032
19. Frazão, C., Camões, A., Barros, J., Gonçalves, D.: Durability of steel fiber reinforced self-compacting concrete. Constr. Build. Mater. **80** (2015). https://doi.org/10.1016/j.conbuildmat.2015.01.061
20. Sedriks, A.J.: Corrosion of Stainless Steel, 2edn. Wiley, New York, NY (United States) (1996)
21. Schunemann, A.C., Mills Gates, Ohio.: Copper coated steel (1967)

22. Hosking, N.C., Ström, M.A., Shipway, P.H., Rudd, C.D.: Corrosion resistance of zinc-magnesium coated steel. Corros. Sci. **49** (2007). https://doi.org/10.1016/j.corsci.2007.03.032
23. Bhutta, A., Farooq, M., Banthia, N.: Performance characteristics of micro fiber-reinforced geopolymer mortars for repair. Constr. Build. Mater. **215** (2019). https://doi.org/10.1016/j.conbuildmat.2019.04.210
24. Castel, A., Foster, S.J.: Bond strength between blended slag and Class F fly ash geopolymer concrete with steel reinforcement. Cem. Concr. Res. **72** (2015). https://doi.org/10.1016/j.cemconres.2015.02.016
25. Ranjbar, N., Mehrali, M., Mehrali, M., et al.: High tensile strength fly ash based geopolymer composite using copper coated micro steel fiber. Constr. Build. Mater. **112** (2016). https://doi.org/10.1016/j.conbuildmat.2016.02.228
26. Alrefaei, Y., Dai, J.G.: Tensile behavior and microstructure of hybrid fiber ambient cured one-part engineered geopolymer composites. Constr. Build. Mater. **184** (2018). https://doi.org/10.1016/j.conbuildmat.2018.07.012
27. Sivakumar, A., Srinivasan, K.: High performance fiber reinforced alkali activated slag concrete. Int. J. Civil Archit. Struct. Construct. Eng. **8**, 1217–1220 (2014)
28. Siddique, R., Khatib, J., Kaur, I.: Use of recycled plastic in concrete: a review. Waste Manag. **28** (2008). https://doi.org/10.1016/j.wasman.2007.09.011
29. Mehrali, M., Bagherifard, S., Akbari, M., et al.: Blending electronics with the human body: a pathway toward a cybernetic future. Adv. Sci. **5** (2018). https://doi.org/10.1002/advs.201700931
30. Ko, Y.H., Ahart, M., Ko, J.H., Song, J.: Investigation of polymorphism for amorphous and semi-crystalline poly (-ethylene terephthalate-) using high-pressure Brillouin spectroscopy. J. Korean Phys. Soc. **70** (2017). https://doi.org/10.3938/jkps.70.382
31. Mwangi, J.P.M.: Flexural Behavior of Sisal Fiber Reinforced Concrete Beams. University of California (2001)
32. Larena, A., Pinto, G.: The effect of surface roughness and crystallinity on the light scattering of polyethylene tubular blown films. Polym. Eng. Sci. **33** (1993). https://doi.org/10.1002/pen.760331204
33. Ranjbar, N., Mehrali, M., Behnia, A., et al.: A comprehensive study of the polypropylene fiber reinforced fly ash based geopolymer. Plos One **11** (2016). https://doi.org/10.1371/journal.pone.0147546
34. Mu, B., Meyer, C., Shimanovich, S.: Improving the interface bond between fiber mesh and cementitious matrix. Cem. Concr. Res. **32** (2002). https://doi.org/10.1016/S0008-8846(02)00715-9
35. Richardson, A.E.: Compressive strength of concrete with polypropylene fiber additions. Struct. Surv. **24** (2006). https://doi.org/10.1108/02630800610666673
36. Banthia, N., Gupta, R.: Influence of polypropylene fiber geometry on plastic shrinkage cracking in concrete. Cem. Concr. Res. **36** (2006). https://doi.org/10.1016/j.cemconres.2006.01.010
37. Ochi, T., Okubo, S., Fukui, K.: Development of recycled PET fiber and its application as concrete-reinforcing fiber. Cem. Concr. Compos. **29** (2007). https://doi.org/10.1016/j.cemconcomp.2007.02.002
38. Redon, C., Li, V.C., Wu, C., et al.: Measuring and modifying interface properties of PVA fibers in ECC matrix. J. Mater. Civ. Eng. **13** (2001). https://doi.org/10.1061/(asce)0899-1561(2001)13:6(399)
39. Li, V.C., Wu, C., Wang, S., et al.: Interface tailoring for strain-hardening polyvinyl alcohol-engineered cementitious composite (PVA-ECC). ACI Mater. J. **99** (2002). https://doi.org/10.14359/12325
40. Nematollahi, B., Qiu, J., Yang, E.H., Sanjayan, J.: Micromechanics constitutive modelling and optimization of strain hardening geopolymer composite. Ceram. Int. **43** (2017). https://doi.org/10.1016/j.ceramint.2017.01.138
41. Zhang, S., Duque-Redondo, E., Kostiuchenko, A., et al.: Molecular dynamics and experimental study on the adhesion mechanism of polyvinyl alcohol (PVA) fiber in alkali-activated slag/fly ash. Cem. Concr. Res. **145** (2021). https://doi.org/10.1016/j.cemconres.2021.106452

42. Kanda, T., Li, V.C.: Interface property and apparent strength of high-strength hydrophilic fiber in cement matrix. J. Mater. Civ. Eng. **10** (1998). https://doi.org/10.1061/(asce)0899-1561(1998)10:1(5)
43. Nematollahi, B., Sanjayan, J., Qiu, J., Yang, E.H.: High ductile behavior of a polyethylene fiber-reinforced one-part geopolymer composite: a micromechanics-based investigation. Arch. Civil Mech. Eng. **17** (2017). https://doi.org/10.1016/j.acme.2016.12.005
44. Zheng, Z.: Synthetic fiber-reinforced concrete. Prog. Polym. Sci. **20**, 185–210 (1995). https://doi.org/10.1016/0079-6700(94)00030-6
45. Choi, J., Lee, B.Y., Ranade, R., et al.: Ultra-high-ductile behavior of a polyethylene fiber-reinforced alkali-activated slag-based composite. Cem. Concr. Compos. **70** (2016). https://doi.org/10.1016/j.cemconcomp.2016.04.002
46. Lu, W., Fu, X., Chung, D.D.L.: A comparative study of the wettability of steel, carbon, and polyethylene fibersby water. Cem. Concr. Res. **28** (1998). https://doi.org/10.1016/S0008-8846(98)00056-8
47. Cooke, T.F.: Inorganic fibers—A literature review. J. Am. Ceram. Soc. **74** (1991)
48. Sun, Q., Li, W.: Inorganic-Whisker-Reinforced Polymer Composites: synthesis, Properties and Applications (2015)
49. Bentur, A., Mindess, S.: Fiber reinforced cementitious composites (2006)
50. Bentur, A., Ben-Bassat, M., Schneider, D.: Durability of glass-fiber-reinforced cements with different alkali-resistant glass fibers. J. Am. Ceram. Soc. **68** (1985). https://doi.org/10.1111/j.1151-2916.1985.tb15298.x
51. Dhand, V., Mittal, G., Rhee, K.Y., et al.: A short review on basalt fiber reinforced polymer composites. Compos. B Eng. **73** (2015). https://doi.org/10.1016/j.compositesb.2014.12.011
52. Giancaspro, J.W.: Influence of Reinforcement Type on the Mechanical Behavior and Fire Response of Hybrid Composites and Sandwich Structures. Rutgers The State University of New Jersey-New Brunswick, New Brunswick (2014)
53. Wei, B., Cao, H., Song, S.: Tensile behavior contrast of basalt and glass fibers after chemical treatment. Mater. Des. **31** (2010). https://doi.org/10.1016/j.matdes.2010.04.009
54. Militký, J., Kovačič, V., Rubnerová, J.: Influence of thermal treatment on tensile failure of basalt fibers. Eng. Fract. Mech. **69** (2002). https://doi.org/10.1016/S0013-7944(01)00119-9
55. Ishikawa, T.: Advances in inorganic fibers. In: Polymeric and Inorganic Fibers, pp. 109–144. Springer, Berlin/Heidelberg (2005)
56. Chung, D.D.L.: Carbon Composites: Composites with Carbon Fibers, Nanofibers, and Nanotubes, 2nd edn. (2016)
57. Bunsell, A.R., Somer, A.: The tensile and fatigue behaviour of carbon fibers. Plast. Rubber Compos. Process. Appl. **18**, 263–267 (1992)
58. Dorey, G.: Carbon fibers and their applications. J. Phys. D Appl. Phys. **20**, 245–256 (1987). https://doi.org/10.1088/0022-3727/20/3/002
59. Bunsell, A.R.: Handbook of Tensile Properties of Textile and Technical Fibers (2009)
60. Chand, S.: Review carbon fibers for composites. J. Mater. Sci. **35**, 1303–1313 (2000). https://doi.org/10.1023/A:1004780301489
61. Rahaman, M.S.A., Ismail, A.F., Mustafa, A.: A review of heat treatment on polyacrylonitrile fiber. Polym. Degrad. Stab. **92** (2007)
62. Matsumoto, T.: Mesophase pitch and its carbon fibers. Pure Appl. Chem. **57** (1985). https://doi.org/10.1351/pac198557111553
63. Peebles, L.H.: Carbon Fibers: formation, Structure, and Properties (2018)
64. Yadav, S.P., Singh, S.: Carbon nanotube dispersion in nematic liquid crystals: an overview. Prog. Mater. Sci. **80** (2016)
65. Byrne, E.M., McCarthy, M.A., Xia, Z., Curtin, W.A.: Multiwall nanotubes can be stronger than single wall nanotubes and implications for nanocomposite design. Phys. Rev. Lett. **103** (2009). https://doi.org/10.1103/PhysRevLett.103.045502
66. Georgakilas, V., Perman, J.A., Tucek, J., Zboril, R.: Broad family of carbon nanoallotropes: classification, chemistry, and applications of fullerenes, carbon dots, nanotubes, graphene, nanodiamonds, and combined superstructures. Chem. Rev. **115** (2015)

67. Ranjbar, N., Mehrali, M., Mehrali, M., et al.: Graphene nanoplatelet-fly ash based geopolymer composites. Cem. Concr. Res. **76** (2015). https://doi.org/10.1016/j.cemconres.2015.06.003
68. Saafi, M., Tang, L., Fung, J., et al.: Graphene/fly ash geopolymeric composites as self-sensing structural materials. Smart Mater. Struct. **23** (2014). https://doi.org/10.1088/0964-1726/23/6/065006
69. Ardanuy, M., Claramunt, J., Toledo Filho, R.D.: Cellulosic fiber reinforced cement-based composites: a review of recent research. Constr. Build. Mater. **79** (2015)
70. Azwa, Z.N., Yousif, B.F., Manalo, A.C., Karunasena, W.: A review on the degradability of polymeric composites based on natural fibers. Mater. Des. **47** (2013)
71. Chen, R., Ahmari, S., Zhang, L.: Utilization of sweet sorghum fiber to reinforce fly ash-based geopolymer. J. Mater. Sci. **49** (2014). https://doi.org/10.1007/s10853-013-7950-0
72. Alshaaer, M., Mallouh, S.A., Al-Kafawein, J., et al.: Fabrication, microstructural and mechanical characterization of Luffa Cylindrical Fiber-Reinforced geopolymer composite. Appl. Clay Sci. **143** (2017). https://doi.org/10.1016/j.clay.2017.03.030
73. Trindade, A.C.C., Borges, P.H.R., de Andrade Silva, F.: Mechanical behavior of strain-hardening geopolymer composites reinforced with natural and PVA fibers. In: Materials Today: Proceedings (2019)
74. Wei, J., Meyer, C.: Degradation mechanisms of natural fiber in the matrix of cement composites. Cem. Concr. Res. **73** (2015). https://doi.org/10.1016/j.cemconres.2015.02.019
75. Zollo, R.F.: Fiber-reinforced concrete: an overview after 30 years of development. Cem. Concr. Compos. **19** (1997)
76. Banthia, N., Nandakumar, N.: Crack growth resistance of hybrid fiber reinforced cement composites. Cem. Concr. Compos. **25** (2003). https://doi.org/10.1016/S0958-9465(01)00043-9
77. Bunsell, A.R.: Introduction to the science of fibers. In: Handbook of Properties of Textile and Technical Fibers (2018)
78. Koenig, A., Wuestemann, A., Gatti, F., et al.: Flexural behaviour of steel and macro-PP fiber reinforced concretes based on alkali-activated binders. Constr. Build. Mater. **211** (2019). https://doi.org/10.1016/j.conbuildmat.2019.03.227
79. Lee, S.J., Yoo, D.Y., Moon, D.Y.: Effects of hooked-end steel fiber geometry and volume fraction on the flexural behavior of concrete pedestrian decks. Appl. Sci. (Switzerland) **9** (2019). https://doi.org/10.3390/app9061241
80. Ranjbar, N., Talebian, S., Mehrali, M., et al.: Mechanisms of interfacial bond in steel and polypropylene fiber reinforced geopolymer composites. Compos. Sci. Technol. **122** (2016). https://doi.org/10.1016/j.compscitech.2015.11.009
81. Ohno, M., Li, V.C.: A feasibility study of strain hardening fiber reinforced fly ash-based geopolymer composites. Constr. Build. Mater. **57** (2014). https://doi.org/10.1016/j.conbuildmat.2014.02.005
82. Bernal, S., de Gutierrez, R., Delvasto, S., Rodriguez, E.: Performance of an alkali-activated slag concrete reinforced with steel fibers. Constr. Build. Mater. **24**,(2010). https://doi.org/10.1016/j.conbuildmat.2007.10.027
83. Provis, J.L., Arbi, K., Bernal, S.A., et al.: RILEM TC 247-DTA round robin test: mix design and reproducibility of compressive strength of alkali-activated concretes. Mater. Struct./Materiaux et Construct. **52** (2019). https://doi.org/10.1617/s11527-019-1396-z
84. Wallah, S.E., Rangan, B.V.: Low-calcium fly ash-based geopolymer concrete: long-term properties (2006)
85. British Standards Institution Concrete.: Complementary British Standard to BS EN 206. Part 1, Method of specifying and guidance for the specifier
86. Kar, A.: Characterizations of concretes with alkali-activated binder and correlating their properties from micro-to specimen level. Graduate Theses, Dissertations, and Problem Reports (2013)
87. di Prisco, M.: fib Bulletin 105. Fiber reinforced concrete. fib. The International Federation for Structural Concrete (2022)

88. Chen, Y., Matalkah, F., Weerasiri, R.R., et al.: Dispersion of fibers in ultra-high-performance concrete. Concr. Int. **39** (2017)
89. Adesina, A.: Performance of fiber reinforced alkali-activated composites—A review. Materialia (Oxf) **12**, 100782 (2020). https://doi.org/10.1016/j.mtla.2020.100782
90. Mehta, P.K., Monteiro, P.J.M.: Concrete: microstructure, Properties, and Materials, 4th edn. (2014)
91. Afroughsabet, V., Biolzi, L., Ozbakkaloglu, T.: High-performance fiber-reinforced concrete: a review. J. Mater. Sci. **51**, 6517–6551 (2016). https://doi.org/10.1007/s10853-016-9917-4
92. Shah, S.P., Rangan, V.: Fiber reinforced concrete properties. ACI J. Proc. **68** (1971). https://doi.org/10.14359/11299
93. Pfyl, T.: Tragverhalten von Stahlfaserbeton. Zürich (2003)
94. Suksawang, N., Wtaife, S., Alsabbagh, A.: Evaluation of elastic modulus of fiber-reinforced concrete. ACI Mater. J. **115** (2018). https://doi.org/10.14359/51701920
95. van Dao, D., Tran, H.V., Ly, H.-B., Le, T.-T.: Calibration of a stress-strain response for geopolymer concrete under axial compressive load. Proc. Inst. Mech. Eng. Part L: J. Mater.: Des. Appl. **236**, 1623–1636 (2022). https://doi.org/10.1177/14644207221075912
96. Abbass, W., Khan, M.I., Mourad, S.: Evaluation of mechanical properties of steel fiber reinforced concrete with different strengths of concrete. Constr. Build. Mater. **168**, 556–569 (2018). https://doi.org/10.1016/j.conbuildmat.2018.02.164
97. Noushini, A., Aslani, F., Castel, A., et al.: Compressive stress-strain model for low-calcium fly ash-based geopolymer and heat-cured Portland cement concrete. Cem. Concr. Compos. **73**, 136–146 (2016). https://doi.org/10.1016/j.cemconcomp.2016.07.004
98. Löfgren, I.: Fiber-reinforced concrete for industrial construction—A fracture mechanics approach to material testing and structural analysis. Doktorsavhandlingar vid Chalmers Tekniska Hogskola (2005)
99. Ramagiri, K.K.: Evaluation of high-temperature, bond, and shrinkage characteristics of alkali-activated binder concrete. Birla Institute of Technology and Science (2021)
100. Midhun, M.S., Rao, T.D.G., Srikrishna, T.C.: Mechanical and fracture properties of glass fiber reinforced geopolymer concrete. Adv. Concr. Construct. **6** (2018). https://doi.org/10.12989/acc.2018.6.1.029
101. Chen, C., Zhang, X., Hao, H.: Dynamic tensile properties of geopolymer concrete and fiber reinforced geopolymer concrete. Constr. Build. Mater. **393**, 132159 (2023). https://doi.org/10.1016/j.conbuildmat.2023.132159
102. Wei, S., Mandel, J.A., Said, S.: Study of the interface strength in steel fiber-reinforced cement-based composites. J. Am. Concr. Inst. **83** (1986). https://doi.org/10.14359/10453
103. Ganesan, N., Indira, P.V., Santhakumar, A.: Engineering properties of steel fiber reinforced geopolymer concrete. Adv. Concr. Construct. **1** (2013). https://doi.org/10.12989/acc2013.1.4.305
104. Kim, S.-W., Jang, S.-J., Kang, D.-H., et al.: Mechanical properties and eco-efficiency of steel fiber reinforced alkali-activated slag concrete. Materials **8**, 7309–7321 (2015). https://doi.org/10.3390/ma8115383
105. Rossi, L., Patel, R.A., Dehn, F.: New analytical models to predict the mechanical performance of steel fiber-reinforced alkali-activated concrete. Struct. Concr. (2024). https://doi.org/10.1002/suco.202301104
106. Aisheh, Y.I.A., Atrushi, D.S., Akeed, M.H., et al.: Influence of polypropylene and steel fibers on the mechanical properties of ultra-high-performance fiber-reinforced geopolymer concrete. Case Stud. Construct. Mater. **17**, e01234 (2022). https://doi.org/10.1016/j.cscm.2022.e01234
107. Zhang, H., Jia, T.C., Sarker, P.K., et al.: Effect of fiber addition on the static and dynamic compressive properties of ambient-cured geopolymer concrete. J. Build. Eng. **58**, 104991 (2022). https://doi.org/10.1016/j.jobe.2022.104991
108. Mundra, S., Bernal, S.A., Criado, M., et al.: Steel corrosion in reinforced alkali-activated materials. RILEM Tech. Lett. **2** (2017). https://doi.org/10.21809/rilemtechlett.2017.39
109. Monticelli, C., Natali, M.E., Balbo, A., et al.: Corrosion behavior of steel in alkali-activated fly ash mortars in the light of their microstructural, mechanical and chemical characterization. Cem. Concr. Res. **80** (2016). https://doi.org/10.1016/j.cemconres.2015.11.001

110. Kainer, K.U.: Basics of metal matrix composites. In: Metal Matrix Composites: custom-made Materials for Automotive and Aerospace Engineering (2006)
111. Choi, J., Song, K., Song, J.K., Lee, B.Y.: Composite properties of high-strength polyethylene fiber-reinforced cement and cementless composites. Compos. Struct. **138** (2016). https://doi.org/10.1016/j.compstruct.2015.11.046
112. Nematollahi, B., Vijay, P., Sanjayan, J., et al.: Effect of polypropylene fiber addition on properties of geopolymers made by 3D printing for digital construction. Materials **11** (2018). https://doi.org/10.3390/ma11122352
113. Panda, B., Tan, M.J.: Experimental study on mix proportion and fresh properties of fly ash based geopolymer for 3D concrete printing. Ceram. Int. **44** (2018). https://doi.org/10.1016/j.ceramint.2018.03.031
114. Panda, B., Chandra Paul, S., Jen Tan, M.: Anisotropic mechanical performance of 3D printed fiber reinforced sustainable construction material. Mater. Lett. **209** (2017). https://doi.org/10.1016/j.matlet.2017.07.123
115. Lyon, R.E., Balaguru, P.N., Foden, A., et al.: Fire-resistant aluminosilicate composites. Fire Mater. **21** (1997). https://doi.org/10.1002/(SICI)1099-1018(199703)21:2%3c67::AID-FAM596%3e3.0.CO;2-N
116. Hammell, J.A., Balaguru, P.N., Lyon, R.E.: Strength retention of fire resistant aluminosilicate-carbon composites under wet-dry conditions. Compos. B Eng. **31** (2000). https://doi.org/10.1016/S1359-8368(99)00072-4
117. Brádaigh, C.M.Ó., Doyle, A., Doyle, D., Feerick, P.J.: Electrically-heated ceramic composite tooling for out-of-autoclave manufacturing of large composite structures. SAMPE J. **47** (2011)
118. Rill, E., Lowry, D.R., Kriven, W.M.: Properties of basalt fiber reinforced geopolymer composites. In: Ceramic Engineering and Science Proceedings (2010)
119. Mills-Brown, J., Potter, K., Foster, S., Batho, T.: The development of a high temperature tensile testing rig for composite laminates. Compos. Part A Appl. Sci. Manuf. **52** (2013). https://doi.org/10.1016/j.compositesa.2013.04.009
120. Masi, G., Rickard, W.D.A., Bignozzi, M.C., van Riessen, A.: The effect of organic and inorganic fibers on the mechanical and thermal properties of aluminate activated geopolymers. Compos. B Eng. **76** (2015). https://doi.org/10.1016/j.compositesb.2015.02.023